

Isolation, structural identification, synthesis, and pharmacological profiling of 1,2-*trans*-dihydro-1,2-diol metabolites of the utrophin modulator ezutromid

Maria Chatzopoulou,¹ Timothy D.W. Claridge,¹ Kay E. Davies,² Stephen G. Davies,¹ David J. Elsey,³ Enrico Emer,¹ Ai M. Fletcher,¹ Shawn Harriman,⁴ Neil Robinson,⁵ Jessica A. Rowley,¹ Angela J. Russell,^{1,6} Jonathon M. Tinsley,³ Richard Weaver,⁷ Isabel V.L. Wilkinson,¹ Nicky J. Willis,¹ Francis X. Wilson,³ and Graham M. Wynne¹*

¹ Department of Chemistry, University of Oxford, Chemistry Research Laboratory, Mansfield Road, Oxford, OX1 3TA, UK

² Department of Physiology, Anatomy and Genetics, MDUK Oxford Neuromuscular Centre, University of Oxford, Oxford, OX1 3PT, UK

³ Summit Therapeutics plc, 136a Eastern Avenue, Milton Park, Abingdon, OX14 4SB, UK

⁴ Summit Therapeutics plc, One Broadway, 14th Floor, Cambridge, MA 02142, US

⁵ S.H.B. Enterprises Ltd, 55 Station Road, Beaconsfield, HP19 1QL

⁶ Department of Pharmacology, University of Oxford, Mansfield Road, Oxford, OX1 3PQ, UK

⁷ XenoGesis Ltd, BioCity Nottingham, Pennyfoot Street, Nottingham, NG1 1GF, UK

KEYWORDS: Duchenne muscular dystrophy, ezutromid, 1,2-dihydrodiol, *beta*-substituted naphthalene metabolism

ABSTRACT

5-(Ethylsulfonyl)-2-(naphthalen-2-yl)benzo[d]oxazole (ezutromid, 1) is a first in class utrophin modulator which has been evaluated in a phase 2 clinical study for the treatment of Duchenne Muscular Dystrophy (DMD). Ezutromid was found to undergo hepatic oxidation of its 2-naphthyl substituent to produce two regioisomeric 1,2-dihydronaphthalene-1,2-diols, DHD1 and DHD3, as the major metabolites after oral administration in humans and rodents. In many patients, plasma levels of the DHD metabolites were found to exceed ezutromid. Herein, we describe the structural elucidation of the main metabolites of ezutromid, the regio- and relative stereochemical assignments of DHD1 and DHD3, their *de novo* chemical synthesis and their production in *in vitro* systems. We further elucidate the likely metabolic pathway and CYP isoforms responsible for DHD1 and DHD3 production and characterise their physicochemical, ADME, pharmacological properties and preliminary toxicological profile.

Introduction

Duchenne muscular dystrophy (DMD) is one of the most prevalent neuromuscular disorders and is caused by mutations on the dystrophin gene that result in loss of the key structural protein dystrophin. This is an essential component of the dystrophin-associated protein complex that connects the actin cytoskeleton to the basal lamina. Loss of dystrophin results in chronic inflammation and a vicious cycle of muscle necrosis and regeneration that leads to the eventual replacement of muscle by adipose and connective tissue. The gradual muscle degeneration causes loss of ambulation in adolescence but ultimately respiratory and cardiac failure, significantly reducing the life expectancy of DMD patients.^{1,2}

Dystrophin is the largest gene known in humans and shows high susceptibility to spontaneous mutations.^{3,4} As a result, DMD patients can have different mutations and this has created a challenge in the design of disease-modifying therapeutics as many are targeted to a specific mutation and thus a sub-population rather than all patients.⁵ Until recently, patients could only be treated with symptomatic therapy like corticosteroids to reduce inflammation; however this is now changing with the conditional approval of ataluren (PTC Therapeutics) for nonsense mutations by the European Medicines Agency (EMA), although it is not yet approved by the FDA. An exon skipping drug, eteplirsen (Sarepta Therapeutics) has also been granted conditional approval by the U.S Food and Drug Administration (FDA). Other disease modifying approaches that are currently under clinical investigation include gene therapy and exon skipping candidates for mutations other than exon 51. For many years we have pursued an alternative disease-modifying approach in DMD: to replace defective dystrophin with utrophin, an approach in principle applicable to all DMD patients irrespective of their mutation.

Utrophin is a structural paralogue of dystrophin discovered and characterised over two decades ago.⁶ Initial proof of principle studies in *mdx* mice^{7, 8} and DMD dog⁹ were encouraging and this data supported the initiation of drug discovery programs from a number of companies.¹⁰ The most advanced small molecule utrophin modulator to date is ezutromid (formerly SMT C1100, Summit Therapeutics plc),¹¹ a first in class utrophin modulator that progressed further, to a Phase 2 clinical trial in DMD boys (PhaseOut DMD). Encouraging interim 24-week data, demonstrated reduced muscle fibre damage and increased levels of utrophin following ezutromid treatment, providing the first evidence of target engagement and proof of mechanism. However, ezutromid failed to meet its primary or secondary endpoints after 48 weeks of treatment and further development was discontinued.¹²

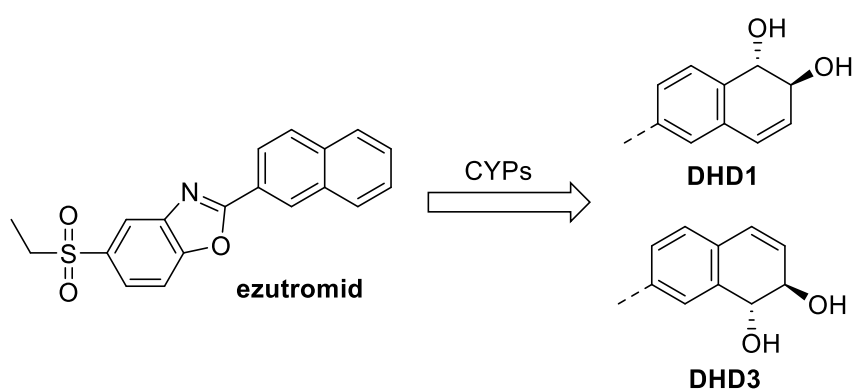


Figure 1. Chemical structure of ezutromid and isolated major metabolites DHD1 and DHD3 (in each case one of two possible enantiomers is drawn as absolute configuration was not determined)

Ezutromid (Figure 1) bears a naphthalene moiety and is extensively metabolised after oral administration.¹³⁻¹⁵ Naphthalene moieties commonly undergo oxidative metabolism: glutathione adducts and naphthols were the first isolated metabolites, both postulated to arise from a common reactive intermediate later identified as the 1,2-naphthalene oxide.^{16, 17} Several CYP isoforms (CYP1A1, CYP1A2, CYP2E1, CYP2F1, CYP3A4, CYP2A6) have been found to produce this

intermediate.¹⁸⁻²¹ 1-Naphthol can be produced by rearrangement of 1,2-naphthalene oxide, while 1,2-dihydro-1,2-diol formation can proceed either by enzymatic or non-enzymatic hydrolysis.^{20,22} In an *in vitro* study in pooled human liver microsomes (HLM), naphthalene was metabolised to predominantly 1,2-dihydrodiol along with 1-naphthol and 2-naphthol, a transformation subsequently found to be mediated predominantly by CYP1A2.²⁰ Similar metabolic pathways have also been observed for 1-naphthalene-containing drugs or investigational drugs such as setipiprant, cinacalcet and terbinafine, but to the best of our knowledge there are no similar reports of 2-naphthalene-containing drug candidates.^{23,24,23-26}

Clinical studies of ezutromid in healthy volunteers and pediatric DMD patients demonstrated two major abundant metabolites in plasma, accounting for >90% of total drug exposure on Day 1 and approximately 70% on Day 11.¹³⁻¹⁵ These were tentatively assigned as regioisomeric 1,2-dihydrodiols and named DHD1 and DHD3 (Figure 1) based on the order of elution in the analytical procedure employed. In urine, species assigned as hydroxylated metabolites of ezutromid and their respective *O*-glucuronides were found. While the plasma concentration of ezutromid varied significantly between subjects, the relative ratios between ezutromid and metabolites were very similar.¹³ Furthermore, exposure to ezutromid was observed to decrease with repeated dosing, while metabolite levels increased. It was therefore important to determine the major route of metabolism of ezutromid and consequent potential CYP induction in order to better understand the compounds PK/PD profile.

Herein, we detail ezutromid's metabolic profile in *in vitro* and *in vivo* systems, together with the structural elucidation and pharmacological characterisation of the major dihydrodiol metabolites DHD1 and DHD3.

Results and Discussion

Ezutromid's metabolism was investigated using a human *in vitro* model. A preliminary study in human liver microsomes (HLM) showed that after incubation for 45 minutes an 81:19 mixture of parent (A) and a single metabolite was observed (B, T_R 5.7 min, $[M+H]^+$ m/z 372, Figures S1, S3). Mass spectrometry analysis showed this metabolite corresponded to an increase of 34 mass units which indicated either addition of H_2O_2 , H_2 and CH_3OH , or H_2S . MS-MS fragmentation analysis (m/z 354, 344, 326, 279 and 261) demonstrated a loss of m/z 18 (H_2O , m/z 354), suggesting a formal addition of H_2O_2 . Key fragments of ezutromid (m/z 310 ($-C_2H_4$) and 245 ($-C_2H_5SO_2$)) were visible as 344 ($-C_2H_4$) and 279 ($-C_2H_5SO_2$) within the MS-MS fragmentation of the metabolite (Figures S2-4) suggesting that this metabolite may be a dihydroxylated benzoxazole or a dihydronaphthalenediol (Figure 2).

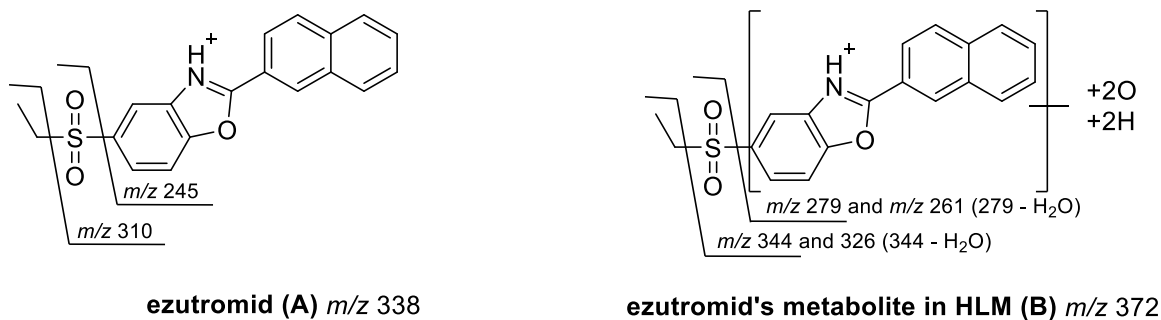


Figure 2. Proposed fragmentation pathway of ezutromid (A) and main metabolite (B) in human liver microsomes (HLM).

A more comprehensive investigation of ezutromid metabolism was accomplished using a single oral administration of a radiolabelled sample of $[^{14}C-1]$ ezutromid in mice. Metabolites and their relative proportions were measured in plasma, urine, faeces and liver over 3 days. A total of 16 metabolites were observed in plasma, up to 19 in excreta and liver and the identities of 14 of them were discerned from a combination of accurate mass measurements and diagnostic MS^n fragments

(Figures S5-9, Tables S1-2). Consistent with the observations in human samples, the most prominent metabolites in excreta were consistent with two isomeric dihydrodiol derivatives of ezutromid (M4 and M8) and their corresponding glucuronide adducts (M2 and M5) (Figure S5, Tables S1-2).

Production of metabolites using *in vitro* systems

A route to larger quantities of ezutromid's metabolites was required in order to elucidate their structure and investigate their pharmacological profiles. Ezutromid stability was investigated in a range of *in vitro* systems in an attempt to identify an appropriate system for production of the DHDs. Ezutromid's metabolism was found to vary significantly between different species *in vitro* (Table S3).

Using MicroCyp enzymes, a recombinant human cytochrome P450 and a microbial biocatalyst panel, failed to produce the desired metabolites in sufficient quantities. Several attempts at a biomimetic approach based on epoxidation followed by hydrolysis also gave only trace quantities of the desired metabolites.

The optimal, most cost-effective and scalable conditions for the synthesis of the major metabolites was found to be by metabolic conversion of ezutromid with induced rat S9 fractions (β -naphthoflavone/phenobarbital) (Table S4). UV-Vis spectroscopy showed conversion to a 18:77:5 mixture of ezutromid, dihydrodiol-1 (**D1**) and dihydrodiol-2 (**D2**) after 4 h of incubation (Figure S10). Though this procedure was low yielding for diol **D2** it was found to be amenable to scale-up: scaling up to 200 mL incubation volume gave similar levels of conversion to **D1** and **D2** (Table S5, Figure S11). The isolated sample of **D1** was compared to the samples produced from the radiochemical study in mice and was found to have similar retention times to M4 (T_R 26.7 and

27.5 min, respectively) and identical fragmentation by MS/MS, suggesting these had the same composition (Figures S12-13, Table S6).

Moreover, the analytical data of dihydrodiol metabolites DHD1 and DHD3 from human plasma samples, were compared to those from induced rat S9 **D1** and **D2** using LC-MS/MS (Figure 3). **D1** eluting at $T_R = 8.2$ min with m/z 372.0898 matched the sample of DHD1 from human patients M372a, $T_R = 8.1$ min with m/z 372.0899. **D2** eluting at $T_R = 9.0$ min with m/z 372.0899 matched the sample of DHD3 from human patients M372b, $T_R = 8.9$ min with m/z 372.0898. Further accurate mass measurement of both samples gave identical fragmentation for the two samples supporting the same composition (Table S7, Figures S14-17).

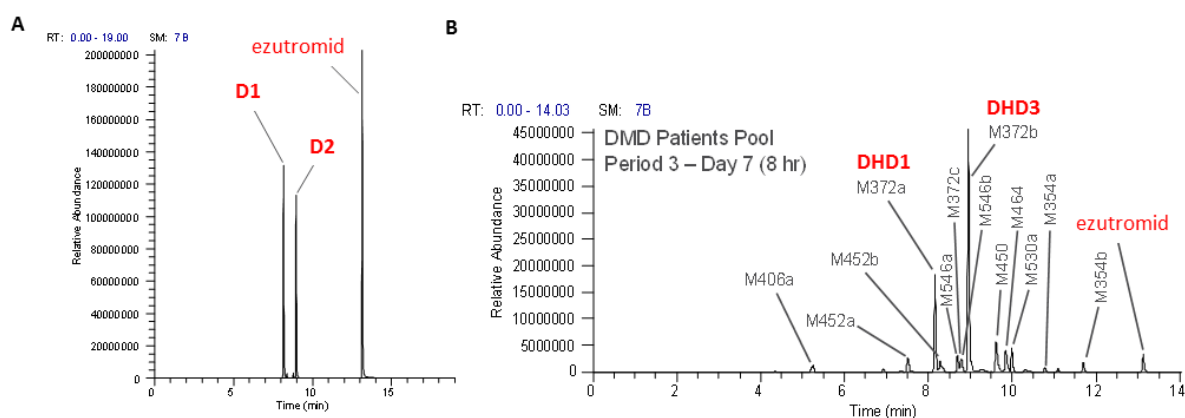
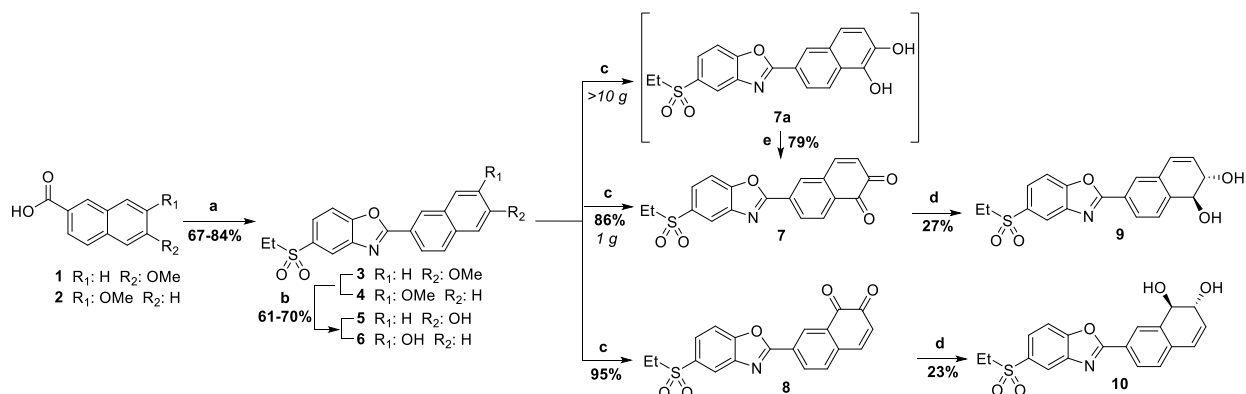


Figure 3. Cumulative accurate mass summed ion chromatograms for: A) an equimolar mixture of ezutromid, **D1**, and **D2** reference standards B) plasma following multiple oral doses of ezutromid (1.0 g, BID) in paediatric DMD subjects – 8 hours post-AM dose on day 7

***De novo* synthesis of dihydrodiols DHD1 and DHD3**

In order to assign the correct regio- and relative stereochemistries to the dihydrodiols DHD1 and DHD3 we carried out a *de novo* chemical synthesis. Several previous studies on 1-naphthyl-

containing molecules report preferential formation of 7,8-dihydrodiol or 5,6-dihydrodiol as the major (or only) metabolites.^{27,28,29-32} Based on the proposed 2-step epoxidation-transdiaxial ring opening mechanism of 1,2-dihydrodiol formation,²⁴ it was envisaged that the relative stereochemistry in both dihydrodiols was likely to be *trans*. Thus, authentic samples of *trans*-dihydrodiols **9** and **10**, reasoned to be the major metabolites from ezutromid, were synthesized from the corresponding naphthalenes (Scheme 1).



Scheme 1. Synthetic route to *trans*-1,2-dihydrodiols **9** and **10** (one of two possible enantiomers is depicted as absolute configuration was not unambiguously determined). Reagents and conditions: (a) (1) SOCl₂, DMF, 1,4-dioxane, 80 °C, 1 h; (2) 2-amino-4-(ethylsulfonyl)phenol, MsOH, p-xylene, 140 °C, 48 h. (b) BBr₃, DCM, 0-40 °C, 24 h. (c) IBX, DMF, rt, 90 min. (d) LiBH₄, O₂, rt, 24 h (e) *o*-chloranil, DMF, rt, 24 h.

Regioisomeric 6-methoxy-2-naphthoic acid **1** and 7-methoxy-2-naphthoic acid **2** were treated sequentially with thionyl chloride, 2-amino-4-(ethylsulfonyl)phenol and BBr₃ to afford naphthols **5** and **6** in good yields (67-84% over three steps). Oxidation of **5** and **6** with IBX gave 5,6-diketo and 7,8-diketo species **7** and **8** respectively. Initial attempts to scale up the production of **9** resulted in either partial oxidation of **5** to naphthalene diol **7a**, or a mixture of **7** and **7a**. However, treatment of **7a** with *o*-chloranil gave complete conversion to the diketo species **7**. Reduction of the diketo-

species to the final dihydrodiol products **9** and **10** was attempted under a range of conditions including NaBH₄, KBH₄, Pd/C, LiAlH₄, LiAlH(OtBu₃)₃, REDAL, DIBAL, in air, under oxygen or an inert atmosphere. Optimal conditions were found to be treatment with LiBH₄ under an oxygen atmosphere. The final products **9** and **10** were isolated as racemic mixtures after chromatography (SI). **9** and **10** were resolved into single enantiomers following chiral chromatography.

Metabolite Structure Determination/Verification

Unambiguous structure elucidation of **D1**/DHD1 and **D2**/DHD3 was achieved with full NMR assignment and comparison with the authentic samples obtained from chemical synthesis. Overlaying of the ¹H-NMR spectra of **9** and **D1** showed complete overlap, similarly overlaying of the spectra of **10** and DHD3 also showed complete overlap (Figures S18-19). Full assignments were based on COSY for *J*-coupled pairs of protons, and edited HSQC and HMBC correlations for the assignments of aromatic, aliphatic carbon-13 chemical shifts and their attached protons. The regiochemistry of both dihydrodiols was assigned by NOESY. For **D1**, determined to be the 6-benzoxazol-2-yl regioisomer, characteristic NOE correlations were observed between H₈ and H₁, and alkene proton H₄ with naphthalene proton H₅ (Figure 4a). In **D2**, determined to be the 7-benzoxazol-2-yl regioisomer, characteristic NOE correlations were observed between H₈ and H₁, and H₅ with alkene proton H₄ (Figure 4b). In both regioisomers a NOE correlation was observed between H₂ and H₃, and no strong NOE correlation was observed between H₁ and H₂, consistent with *trans* relative stereochemistry in both cases. The observed H₁-H₂ cross peak is dominated by scalar coupling effects, with evidence of only a very weak NOE between the protons contributing to it. The assignment of *trans* relative stereochemistry was further supported by analysis of vicinal coupling constants in the ¹H-NMR spectra: for both **D1** and **D2** ³J_(H1,H2) = 10.5 Hz (³J_(H2,H3) = 2.4

Hz). This is consistent with data for other reported *trans*-dihydrodiols,³³ while *cis*-dihydrodiols have much lower recorded *J* values (i.e 4.8 Hz).³⁴

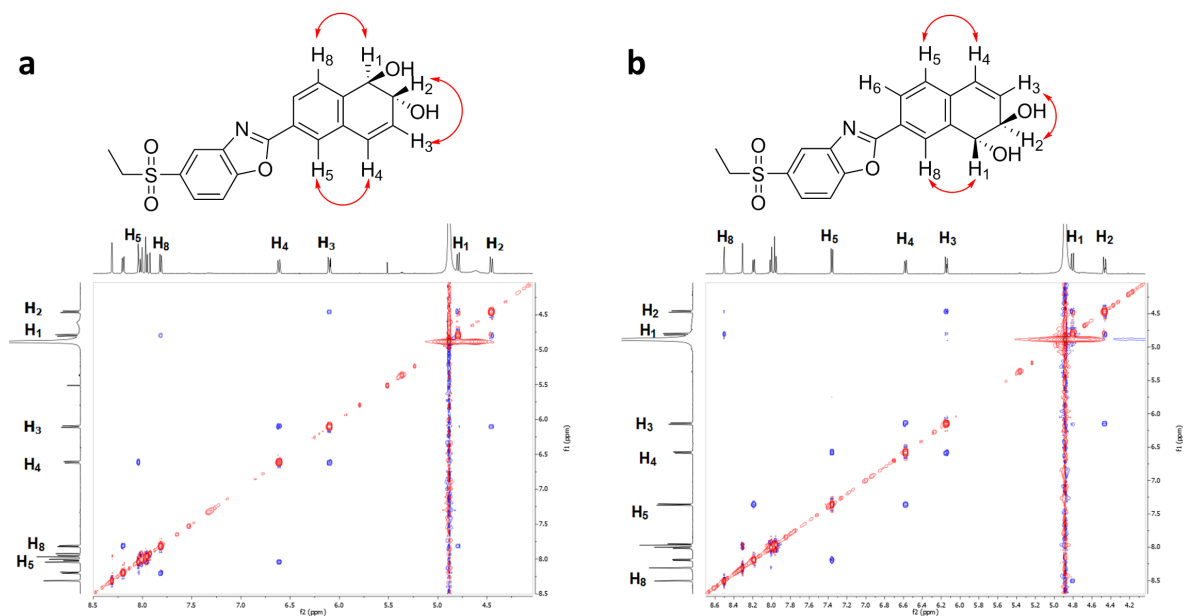


Figure 4. NOESY spectra and NOE correlations for structure elucidation of a) **D1** and b) **D2**. One of two possible enantiomers is shown, absolute configuration was not determined.

Determination of CYP-mediated metabolism of ezutromid

Naphthalene has been shown to be predominantly metabolised by human CYP1A2 into the *trans*-1,2-dihydrodiol and to the 1-naphthol. CYP3A4 has also shown to induce metabolism to the 2-naphthol.²⁰ To identify the main CYP isoforms involved in ezutromid's metabolism two approaches were employed. Firstly, a panel of 8 recombinant CYP isoform expression systems (Bactosomes™) were incubated with ezutromid (Table S8). Secondly, CYP isoform specific chemical inhibitors were used to determine their effects on ezutromid metabolism in human liver microsomes (Table S9).

The shortest half-life for ezutromid was observed in the presence of CYP1A1 ($T_{1/2}$ 2.16 min) and CYP1A2 ($T_{1/2}$ 2.62 min) bactosomes (Table S8). Turnover of ezutromid in CYP2B6, CYP2C8,

CYP2C9, CYP2C19, CYP2D6 and CYP3A4 bacosomes was minimal ($T_{1/2} \geq 180$ min). Formation of DHD1 was observed upon incubation of ezutromid with CYP1A2, CYP2B6 and CYP2D6 although peak area ratios were small. Formation of DHD3 was not observed under any conditions.

In human liver microsomes, turnover of ezutromid was decreased in the presence of inhibitors of CYP1A (CL_{int} 5.06 $\mu\text{L}/\text{min}/\text{mg}$), CYP2B6 (CL_{int} 21.37 $\mu\text{L}/\text{min}/\text{mg}$) and CYP2D6 (CL_{int} 35.1 $\mu\text{L}/\text{min}/\text{mg}$) compared to control (CL_{int} 50.67 $\mu\text{L}/\text{min}/\text{mg}$) (Table S9). Ticlopidine was used as an FDA recommended inhibitor for CYP2B6, however it has been shown to inhibit other CYP isoforms, including CYP1A2, at the concentration used in this study. It was therefore plausible, and consistent with our observations of CYP1A1/2-mediated metabolism of ezutromid in bacosomes, that the decrease in turnover of ezutromid in the presence of ticlopidine might result from CYP1A2 inhibition rather than CYP2B6. This was further supported by the observation that decreased formation of both DHD1 and DHD3 was observed only in the presence of inhibitors of CYP1A (6% and 11% of control) and to a lesser extent CYP2D6 (65% and 66% of control). The CYP2D6 inhibitor used, quinidine, has been reported to be a relatively selective inhibitor, inhibiting CYP3A4 only at higher concentrations ($IC_{50} = 28 \mu\text{M}$),^{35, 36} thus CYP2D6 appears to also be involved in ezutromid's metabolism, but to a lesser extent than CYP1A1/2.

In summary, the CYP1A1 and CYP1A2 enzymes appear to be the main P450 isoforms mediating ezutromid's metabolism and the formation of DHD1 and DHD3 *in vitro*. Based on the methods used, CYP2C8, CYP2C9, CYP2C19 and CYP3A4 do not appear to be involved in the metabolism of this molecule, but CYP2D6 may also contribute to a lesser extent.

Ezutromid metabolite profiling upon repeated dosing

As there was a marked decrease in exposure after repeated dosing of ezutromid in DMD patients,¹⁴ the metabolic profile of ezutromid was investigated in rat after 1 and 28 days (2000 mg/kg). Consistent with the results from DMD patients, it was found that ezutromid's clearance was higher after 28 days of dosing compared to day 1. After 24 hours, notable levels of ezutromid (38-89%) were found in plasma (Table S10). A large variation in the extent of ezutromid metabolism was observed between animals. The most abundant metabolite observed (T_R 4.57-4.61 min, 8-44%) was a dihydrodiol (I) followed by an isomeric dihydrodiol (II) (T_R 4.98-5.00 min, 3-14%).

After 28 days of dosing, more extensive metabolism of ezutromid was observed (Table S11). Ezutromid was detected at low levels and the two main metabolites were found in similar proportions to day 1 [T_R 4.57-4.61 (50-70%), T_R 4.98-5.00 min (10-12%), dihydrodiol I and II respectively]. Two other metabolites were also present in significant amounts, a glucuronide conjugate of a dihydrodiol, and the O-glucuronide conjugate of an aromatised diol. In urine, the composition of metabolites changed significantly with dihydrodiol glucuronides being the most abundant (Table S12). The relative proportions of the remaining metabolites varied significantly between male and female rats.

CYP Induction

As exposure to ezutromid was observed to decrease over time with a concurrent increase in the levels of metabolites in both humans and rodents,¹³ the propensity of ezutromid and its two major metabolites DHD1 and DHD3 to induce CYP expression was investigated. No significant induction of CYP1A1/2 was observed using *in vitro* systems where only a single dose was administered: after 48 h incubation of ezutromid (0.1-10 μ M) with rat hepatocytes no significant

difference in CYP1A1/2 mediated enzyme activity was observed (data not shown). Similarly, in human hepatocytes, incubation with ezutromid for 48 h did not result in significant induction of CYP1A2 (data not shown). However, ezutromid was observed to inhibit CYP1A2 enzymic activity in human liver microsomes with an IC_{50} of 5.4 μ M.

Although no evidence in support of CYP induction *in vitro* was observed, a marked elevation in 7-ethoxyresorufin O-deethylase (EROD) activity was observed after treatment with ezutromid (2000 mg/kg/day, p.o) for 28 days in rats. EROD enzyme activity was elevated 17-18 fold, 21-22 fold, and 13-18 fold when expressed per mg protein, per g liver and per nmole P450, respectively (Table S13). No significant changes were observed in microsomal protein or total P450 concentration. EROD activity is used as a proxy for induction of the CYP1A subfamily (CYP1A1, CYP1A2);³⁷ thus these data suggest that repeated oral administration of ezutromid in rats can result in induction of CYP1A, which are the principal enzymes responsible for mediating metabolism of ezutromid.

A similar trend was observed after administration of ezutromid (500 mg/kg/day) for 39 weeks in minipigs. No evidence of significant increase in microsomal protein concentration and total cytochrome P450 content were observed (data not shown), but a small increase in EROD and 7-pentoxyresorufin O-depentylase (PROD) activity (2.1 fold and 2.0 fold, respectively) was observed in female minipigs (Table S14). The magnitude of this effect was very low in comparison to that observed with other CYP1A and CYP2B inducers. The marked gender difference between the basal levels of CYP1A activity in minipigs (CYP1A2 and CYP2B activity is higher in female minipigs by 4- and 3.8-fold respectively),³⁸ could account for the observed lack of increased EROD or PROD activity in male minipigs. No effect was observed on testosterone hydroxylase, lauric

acid 11- and 12-hydroxylase activity, suggesting no induction of CYP3A, CYP2E1 and CYP4A respectively.

Pharmacological characterisation and *in vitro* PK profiling of DHD1 and DHD3

As the two major metabolites DHD1 and DHD3 were produced in significant amounts *in vivo*, and exposure exceeded that of ezutromid in some patients,¹⁵ a systematic analysis of the pharmacological activity, physicochemical properties, pharmacokinetic and toxicological profile of DHD1 and DHD3 was undertaken.

Although both metabolites appeared to show comparable levels of activity to ezutromid in the H2K-*mdx* utrA-luc assay,³⁹ a luciferase reporter gene assay using a human muscle specific utrophin A promoter in mouse *mdx* myoblasts, differences were observed in the Homogenous Time-Resolved Fluorescence (HTRF) assay quantifying human utrophin protein in cell lysates of iDMC cells (Table 1). In the latter assay, no increase in utrophin protein was observed upon treatment with DHD1 up to the highest concentration tested (10 μ M), while DHD3 was found to increase utrophin protein but with an approximately 6-fold reduction in potency compared to ezutromid. The molecular target of ezutromid and the mechanism through which it increases utrophin protein levels is not yet known, and so it is unclear at this stage whether DHD3 and ezutromid act through a common molecular target or distinct pathways leading to an increase in utrophin protein. Studies are ongoing to resolve this question.

Table 1. Assay data to monitor for utrophin upregulation for DHD1 and DHD3 metabolites of ezutromid

Compound	H2K ^a EC ₅₀ \pm SEM ^b (μ M)	HTRF ^c EC ₅₀ \pm SEM ^d (μ M)
DHD1	0.37 \pm 0.08	>10 μ M

DHD3	0.12 ± 0.03	8.35 ± 0.62
ezutromid	0.11 ± 0.01	1.28 ± 0.24

^a firefly luciferase reporter gene assay in H2K-*mdx* utrA-luc cells; ^b EC₅₀ values were calculated using non-linear regression (curve fit) from 2 biological replicates (3 technical replicates each); ^c HTRF, homogenous time-resolved fluorescence assay; ^d EC₅₀ values were calculated using non-linear regression (curve fit) from 2 biological replicates (3 technical replicates each)

Physicochemical and *in vitro* PK properties were also determined for DHD1 and DHD3 (Tables 2-3). Both metabolites had a measured logD of around 2, with increased solubility and permeability, and a higher unbound fraction to mouse and human plasma proteins compared to ezutromid (Table 2). Metabolic stability was measured *in vitro* in mouse and human S9 fractions and hepatocytes. DHD3 was found to be the more stable of the two metabolites in both mouse and human hepatocytes (Table 3).

Table 2. Physicochemical profile and plasma protein binding (100% plasma) of DHD1 and DHD3 metabolites of ezutromid

Compound	logD (pH 7.4)	KinSol (μM)	PAMPA _{pH 7.4} (10 ⁻⁶ cm/s)	PPB F _b (%)	
				mouse	human
DHD1	2.04	96	33.3	Highly unbound	63.7
DHD3	1.95	210	34.4	92.3	87.2
ezutromid	ND	1-2	9.5	99.5	99.0

Abbreviations: F_b, fraction bound; KinSol, kinetic aqueous solubility; PAMPA, parallel artificial membrane permeability assay; PPB, plasma protein binding

Table 3. *In vitro* metabolic stability of DHD1 and DHD3 metabolites of ezutromid in mouse and human microsomes (S9 fraction) and hepatocytes (Hep)

Compound	$T_{1/2} \pm \text{SD (min)}$				$\text{CL}_{\text{int}} \pm \text{SD } (\mu\text{L/min.mg})$			
	mouse		human		mouse		human	
	S9	Hep	S9	Hep	S9	Hep	S9	Hep
DHD1	39 \pm 1.8	7 \pm 0.7	>138	85 \pm 8.2	35 \pm 1.3	98 \pm 9.9	<10	8 \pm 0.8
DHD3	112 \pm 26.2	143 \pm 16.3	>138	142 \pm 10.3	13 \pm 3.1	5 \pm 0.6	<10	5 \pm 0.4
ezutromid	74 \pm 7.8		101 \pm 4.5		19 \pm 2.0		14 \pm 0.6	

Preliminary toxicology and safety assessment of metabolites

UGT turnover and UGT inhibition by ezutromid metabolites

No detectable turnover of DHD1 and DHD3 was observed in all uridine glucuronate transferase (UGT) incubations ($T_{1/2} > 240$ min). The CL_{int} for both DHD1 and DHD3 with all UGT enzymes was determined to be $< 5.8 \mu\text{L/min/pmol}$, for UGT1A4 it was determined to be $< 2.9 \mu\text{L/min/pmol}$. The propensities of DHD1 and DHD3 to act as UGT inhibitors were also investigated. DHD1 was found to be an inhibitor of UGT1A9 and UGT1A3 (12% and 62% residual activity respectively at $10 \mu\text{M}$ for DHD1); DHD3 was found to be a weak inhibitor of UGT1A9, UGT1A3 and UGT1A4 (45, 79 and 84% residual activity respectively at $10 \mu\text{M}$ for DHD3, Table S15).

Interactions of ezutromid metabolites with liver transporter proteins

The potential of DHD1 and DHD3 to cause drug-induced liver injury was evaluated by screening them against a panel of hepatic transporters *in vitro* (Table S16). Both metabolites were found to inhibit the breast cancer resistance protein (BCRP) efflux transporter with an IC_{50} value in the low micromolar range, and the organic anion transporter protein (OATP) uptake receptors OATP1B1 and OATP1B3 with IC_{50} values in the mid micromolar range. DHD1 was also observed to inhibit

the multidrug and toxic compound extrusion (MATE) transporter 1 with an IC₅₀ value of 10 µM (Table S16). No other interactions were observed. DHD1 and DHD3 were also assessed as substrates for BCRP, MDR1, MDR4, OAT1B1 and OAT1B3. No evidence of transport or uptake was observed for either metabolite (Table S16).

Secondary pharmacology of ezutromid metabolites

DHD1 and DHD3 were screened at 10 µM against a panel of 87 receptors and enzymes (CEREP). No significant interactions were noted with DHD3, but DHD1 was found to inhibit monoamino oxidase B (MAO-B) and the adenosine transporter (Graph S1, Table S17). In a follow up study, DHD1 was found to inhibit MAO-B and the adenosine transporter with IC₅₀ values of 4.0 µM, and 3.9 µM respectively.

Conclusions

The metabolic fate of ezutromid was evaluated using *in vitro* and *in vivo* systems. Hepatic clearance was found to be the main route of ezutromid's metabolism. Oxidative metabolism, predominantly mediated by CYP1A led to the formation of 1,2-dihydrodiols DHD1 and DHD3, produced as the two major metabolites in mice, rats and minipigs, consistent with observations in human plasma. Comparison of analytical and spectroscopic data of DHD1 and DHD3, the dihydrodiol metabolites produced from mice and authentic samples accessed through chemical synthesis allowed the regio- and stereochemical assignment of the structures of both metabolites. While the metabolic fate of 1-substituted naphthalene containing drugs have been profiled, this study provides an insight into the metabolic fate of a 2-substituted naphthalene in mammals and humans, which are less well exemplified in the literature.

The pharmacological, pharmacokinetic and toxicological profile of the two metabolites DHD1 and DHD3 were investigated. Both appear to be equipotent to ezutromid in the luciferase reporter gene assay, however DHD3 was found to be 6-fold less potent compared to ezutromid in an HTRF assay monitoring increases in utrophin protein levels. DHD1 was inactive in the HTRF assay. The physicochemical and *in vitro* pharmacokinetic properties of DHD1 and DHD3 were shown to be more favourable than ezutromid; they showed improved solubility, permeability, metabolic stability, and reduced plasma protein binding. DHD1 or DHD3 were found to have an acceptable toxicological profile: no significant interactions with hepatic transporters or other receptors, ion channels or enzymes were observed for either metabolite.

Experimental Section

General procedures. All reactions involving moisture-sensitive reagents were carried out under a nitrogen or argon atmosphere using standard vacuum line techniques and glassware that was flame dried and cooled under nitrogen before use. Water was purified by an Elix® UV-10 system. All other reagents were used as supplied (analytical or HPLC grade) without prior purification. Thin layer chromatography was performed on aluminium plates coated with 60 F254 silica. Flash column chromatography was performed either on Kieselgel 60 silica on a glass column, or on a Biotage SP4 automated flash column chromatography platform. Melting points were recorded on a EZ-Melt Automated Melting Point Apparatus (EZ Melt) and are uncorrected. NMR spectra were recorded on Bruker Avance III spectrometers (at 400 or 500 MHz) using the deuterated solvent stated and at rt. The field was locked by external referencing to the relevant deuterium resonance. Optical rotations were recorded on a Perkin-Elmer 241 polarimeter with a water-jacketed 1 cm cell. Specific rotations are reported in 10^{-1} deg cm² g⁻¹ and concentrations in g/100 mL. Accurate

mass measurements were run on either a Bruker MicroTOF internally calibrated with polyalanine, or a Micromass GCT instrument fitted with a Scientific Glass Instruments BPX5 column (15 m × 0.25 mm) using amyl acetate as a lock mass. The purity of the final compounds was determined by high performance liquid chromatography (HPLC). Purity was found to be 95% or higher (SI). An EnVision™ 2103 Multilabel plate reader – Perkin Elmer: 620 and 665nm emission filters was used for the HTRF assay. Experiments conducted in CROs used their standard equipment.

The 28 day oral (gavage) administration of ezutromid study in the rat and the 39 week oral (gavage) administration of ezutromid study in minipig were designed to meet the known requirements of European Directive 2001/83/EC and all subsequent amendments together with any relevant International Conference on Harmonisation (ICH) guidelines.

Materials. The starting material for DHD1 (7-methoxy-2-naphthoic acid) was provided by Synthesis Med Chem Pty Ltd; [¹⁴C]ezutromid was synthesised at Covance Laboratories Ltd (synthetic scheme and analytical data reported in SI, Scheme S1). Liver and intestine microsomes for intrinsic clearance of ezutromid were obtained from Xenotech: human microsomes (pooled and mixed gender), monkey microsomes (Cynomolgus, pooled male), dog microsomes (Beagle, pooled male), rat microsomes (Sprague-Dawley, pooled male); pooled human liver microsomes (pooled male and female) for the *in vitro* metabolite identification study in human liver microsomes were prepared at Cypotex. Microsomes were stored at -80°C prior to use; β -naphthoflavone/phenobarbital induced rat S9 was obtained from Xenotech (Product No: R1081.S9, Lot No: 710507 (day 1) and Lot No: 1510257 (days 2-5)); UltraPool™ human liver microsomes 150 were used in the P450 time-dependent inhibition and UGT phenotyping and inhibition studies.

Metabolite extractions from induced rat S9

In brief, ezutromid (100µg/ml), was incubated with β -naphthoflavone/phenobarbital induced rat S9 [0.5mg/ml protein concentration] and NADPH (3 mM) for 7 h. The mixture was then quenched with ice-cold methanol, centrifuged to remove excess protein and solvents were removed. After chiral separation (Reach separations, complete method described in SI), 120 mg D1 and 11 mg D2 were obtained from 188 mg of ezutromid.

D1

^1H NMR (400 MHz, MeOH- d_4) δ 8.29 (dd, $J = 1.8, 0.6$ Hz, 1H), 8.18 (dd, $J = 8.0, 1.8$ Hz, 1H), 8.01 (dd, $J = 7.2, 1.8$ Hz, 1H), 7.98 (d, $J = 1.8$ Hz, 1H), 7.94 (dd, $J = 8.5, 0.7$ Hz, 1H), 7.79 (dd, $J = 7.9, 1.2$ Hz, 1H), 6.59 (dd, $J = 9.9, 2.3$ Hz, 1H), 6.08 (dd, $J = 9.8, 2.4$ Hz, 1H), 4.77 (dd, $J = 10.5, 1.2$ Hz, 1H), 4.43 (dt, $J = 10.5, 2.4$ Hz, 1H), 3.29 (q, $J = 7.4$ Hz, 2H), 1.26 (t, $J = 7.4$ Hz, 3H). ^{13}C NMR (125.5 MHz, MeOH- d_4) δ 166.8, 155.2, 143.7, 136.9, 135.1, 134.2, 128.2, 127.4, 126.8, 126.7, 126.3, 121.5, 112.9, 75.5, 73.7, 51.6, 7.7. $[\alpha_D^{25}] - 46.8$ [c 0.1, MeOH].

D2

^1H NMR (500 MHz, MeOH- d_4) δ 8.48 (d, $J = 1.6$ Hz, 1H), 8.33 – 8.27 (m, 1H), 8.17 (ddd, $J = 7.9, 1.9, 0.8$ Hz, 1H), 7.98 (dd, $J = 8.5, 1.8$ Hz, 1H), 7.94 (dd, $J = 8.5, 0.6$ Hz, 1H), 7.34 (d, $J = 7.9$ Hz, 1H), 6.56 (dd, $J = 9.8, 2.3$ Hz, 1H), 6.13 (dd, $J = 9.8, 2.5$ Hz, 1H), 4.78 (dd, $J = 10.5, 1.3$ Hz, 1H), 4.45 (dt, $J = 10.5, 2.4$ Hz, 1H), 3.29 (s, 2H), 1.26 (t, $J = 7.4$ Hz, 3H). ^{13}C NMR (125.5 MHz, MeOH- d_4) δ 166.9, 155.2, 143.8, 140.0, 138.3, 136.9, 135.6, 128.6, 128.0, 127.6, 126.7, 126.1, 121.5, 112.8, 75.2, 73.9, 51.6, 7.7; $[\alpha_D^{25}] - 177.5$ [c 0.1, MeOH]

Chemistry

General method for the synthesis of naphthols

To a solution of **1** or **2** (3.0 g, 14.8 mmol) in 1,4-dioxane (20 mL), DMF (0.1 mL) and SOCl₂ (2.0 mL, 26.4 mmol) were added dropwise and refluxed for 1 h. The solvents were evaporated and the crude material was used in the next step.

6-Methoxy-2-naphthoyl chloride

¹H NMR (400 MHz, CDCl₃) δ 8.67 (d, J = 2.0 Hz, 1H), 8.03 (dd, J = 8.7, 1.9 Hz, 1H), 7.90 (d, J = 9.0 Hz, 1H), 7.79 (d, J = 8.7 Hz, 1H), 7.24 (s, 1H), 7.17 (d, J = 2.5 Hz, 1H), 3.97 (s, 3H).

7-Methoxy-2-naphthoyl chloride

¹H NMR (400 MHz, CDCl₃) δ 8.64 (dt, J = 1.8, 0.7 Hz, 1H), 7.92 (dd, J = 8.6, 1.9 Hz, 1H), 7.84 (d, J = 8.7 Hz, 1H), 7.80 (d, J = 8.8 Hz, 1H), 7.33 (dd, J = 8.9, 2.5 Hz, 1H), 7.28 (d, J = 2.5 Hz, 1H), 3.96 (s, 3H).

A solution of the crude naphthoyl chloride (14.8 mmol) and 2-amino-4-(ethylsulfonyl)phenol (1.5 g, 14.8 mmol) was refluxed in *p*-xylene for 1 h. Then MsOH (0.15 mL) was added and refluxed for 2 d. The reaction was cooled to room temperature and partitioned between EtOAc (2 x 100 mL) and sat. aq. NaHCO₃ (100 mL), washed with brine (100 mL) and dried over MgSO₄. The crude material was used in the next step.

5-(Ethylsulfonyl)-2-(6-methoxynaphthalen-2-yl)benzo[*d*]oxazole (3)

¹H NMR (400 MHz, CDCl₃) δ 8.73 – 8.69 (m, 1H), 8.33 (d, J = 1.6 Hz, 1H), 8.26 (dd, J = 8.5, 1.7 Hz, 1H), 7.93 (dd, J = 8.5, 1.8 Hz, 1H), 7.88 (t, J = 9.0 Hz, 2H), 7.75 (d, J = 8.4 Hz, 1H), 7.24 (dd, J = 8.9, 2.5 Hz, 1H), 7.19 (d, J = 2.5 Hz, 1H), 3.97 (s, 3H), 3.19 (q, J = 7.4 Hz, 2H), 1.31 (t, J = 7.4 Hz, 3H); ¹³C NMR (125.5 MHz, CDCl₃) δ 166.0, 159.8, 154.0, 143.1, 137.0, 135.3, 130.8, 128.9, 128.4, 127.9, 125.3, 124.7, 121.2, 120.9, 120.3, 111.4, 106.1, 55.6, 51.2, 7.8.

5-(Ethylsulfonyl)-2-(7-methoxynaphthalen-2-yl)benzo[*d*]oxazole (4)

^1H NMR (400 MHz, CDCl_3) δ 8.67 (d, J = 1.7 Hz, 1H), 8.34 (dd, J = 1.8, 0.6 Hz, 1H), 8.13 (dd, J = 8.5, 1.7 Hz, 1H), 7.93 (dd, J = 8.5, 1.8 Hz, 1H), 7.90 (d, J = 8.5 Hz, 1H), 7.81 – 7.76 (m, 1H), 7.74 (dd, J = 8.4, 0.6 Hz, 1H), 7.29 – 7.20 (m, 2H), 3.94 (d, J = 8.3 Hz, 3H), 3.19 (q, J = 7.4 Hz, 2H), 1.31 (t, J = 7.4 Hz, 3H).

BBr_3 (1.0 M in CH_2Cl_2 , 43.6 mL, 43.6 mmol) was added dropwise to **3** or **4** at 0 °C and the reaction was warmed to 40 °C. After 24 h, the reaction was cooled at 0 °C and quenched with water, followed by extractions with $\text{CHCl}_3/\text{iPrOH}$ (3:1, 3 x 50 mL), dried over MgSO_4 , and the solvents were evaporated *in vacuo*. The residue was triturated with ether to obtain 4.43 g of **5** (84% yield over 3 steps) or 3.41 g of **6** (67% yield over 3 steps). Both procedures were scaled up to 25 g with minor changes in yield (61% and 70% for **5** and **6** respectively).

6-(5-(Ethylsulfonyl)benzo[*d*]oxazol-2-yl)naphthalen-2-ol (5)

^1H NMR (500 MHz, $\text{DMSO}-d_6$) δ 10.26 (s, 1H), 8.76 (d, J = 1.8 Hz, 1H), 8.29 (d, J = 1.9 Hz, 1H), 8.16 (dd, J = 8.7, 1.8 Hz, 1H), 8.08 (d, J = 4.0 Hz, 1H), 8.06 (d, J = 4.2 Hz, 1H), 7.94 (dd, J = 8.5, 1.8 Hz, 1H), 7.92 (d, J = 8.7 Hz, 1H), 7.24 (d, J = 2.4 Hz, 1H), 7.22 (dd, J = 8.7, 2.4 Hz, 1H), 3.39 (q, J = 7.3 Hz, 2H), 1.13 (t, J = 7.3 Hz, 3H). ^{13}C NMR (125.5 MHz, $\text{DMSO}-d_6$) δ 165.2, 157.8, 153.2, 142.2, 136.7, 135.3, 131.1, 128.6, 127.3, 127.1, 125.1, 123.9, 120.0, 119.7, 111.8, 109.0, 49.5, 7.3. HRMS (ESI): $[\text{M} - \text{H}]^-$ 352.06438 (error: -1.45 ppm)

7-(5-(Ethylsulfonyl)benzo[*d*]oxazol-2-yl)naphthalen-2-ol (6)

mp 273-275 °C; ^1H NMR (500 MHz, $\text{DMSO}-d_6$) δ 10.07 (s, 1H), 8.65 (d, J = 1.6 Hz, 1H), 8.32 (d, J = 1.8 Hz, 1H), 8.08 (d, J = 8.5 Hz, 1H), 8.03 (dd, J = 8.5, 1.7 Hz, 1H), 8.00 (d, J = 8.6 Hz, 1H), 7.96 (dd, J = 8.5, 1.8 Hz, 1H), 7.89 (d, J = 8.8 Hz, 1H), 7.39 (d, J = 2.4 Hz, 1H), 7.25 (dd, J = 8.8, 2.4 Hz, 1H), 3.40 (q, J = 7.3 Hz, 2H), 1.14 (t, J = 7.3 Hz, 3H). ^{13}C NMR (125.5 MHz,

DMSO-*d*₆) δ 165.5, 156.9, 153.7, 142.5, 135.9, 134.7, 130.0, 129.8, 129.4, 127.2, 125.8, 123.6, 121.7, 120.9, 120.4, 112.4, 110.4, 50.0, 7.7. HRMS (ESI): [M + H]⁺ 354.07916 (error: -0.83 ppm)

General method for the synthesis of diols

To a stirred solution of **5** or **6** (1.0 g, 2.8 mmol) in DMF (10 mL) under a N₂ atmosphere stabilised IBX (800 mg, 2.8 mmol) was added portionwise at 0 °C. The resulting mixture was stirred at rt for 48 h and then Et₂O (5 mL) was added. The mixture was filtered and rinsed with Et₂O (10 mL). The collected orange solid was re-dissolved with iPrOH/CHCl₃ (1:3, 400 mL), washed with sat. aq. NaHCO₃ (200 mL), dried over MgSO₄ and concentrated *in vacuo* to give a bright orange solid (1.05 g, quant). Scale up to 20 g gave the two products in very good to excellent yields (86% and 95% for **7** and **8**, respectively).

6-(5-(Ethylsulfonyl)benzo[*d*]oxazol-2-yl)naphthalene-1,2-dione (**7**)

¹H NMR (400 MHz, CDCl₃) δ 8.43 – 8.39 (m, 1H), 8.33 (d, *J* = 1.6 Hz, 1H), 8.31 (d, *J* = 8.1 Hz, 1H), 8.05 – 8.00 (m, 2H), 7.82 (dd, *J* = 8.6, 0.6 Hz, 1H), 7.60 (d, *J* = 10.1 Hz, 1H), 6.59 (d, *J* = 10.2 Hz, 1H), 3.20 (q, *J* = 7.4 Hz, 2H), 1.33 (t, *J* = 7.4 Hz, 3H).

7-(5-(Ethylsulfonyl)benzo[*d*]oxazol-2-yl)naphthalene-1,2-dione (**8**)

¹H NMR (400 MHz, CDCl₃) δ 8.98 (d, *J* = 1.8 Hz, 1H), 8.58 (dd, *J* = 7.9, 1.8 Hz, 1H), 8.39 (dd, *J* = 1.8, 0.6 Hz, 1H), 8.00 (dd, *J* = 8.6, 1.8 Hz, 1H), 7.81 (d, *J* = 8.8 Hz, 1H), 7.61 (d, *J* = 8.0 Hz, 1H), 7.56 (d, *J* = 10.1 Hz, 1H), 6.60 (d, *J* = 10.1 Hz, 1H), 3.20 (q, *J* = 7.4 Hz, 2H), 1.32 (t, *J* = 7.4 Hz, 3H).

The residue of **7** or **8** (1.05 g, 2.8 mmol) was suspended in EtOH (50 mL) under an O₂ atmosphere and LiBH₄ (0.25 g, 11.3 mmol) was added at 0 °C. The resultant mixture was stirred at rt for 24 h. The solvents were evaporated *in vacuo* and the resulting residue was then partitioned between H₂O (250 mL) and DCM/EtOAc (1:1, 250 mL × 2), dried over Na₂SO₄ and concentrated

in vacuo. Obtained 283 mg **9** and 242 mg **10** (27% and 23% yield, for **9** and **10**, respectively) as crude material for further chromatographic purification *vide infra*.

The last step was not scaled up significantly, and it was run up to 2.5 g scale. For this reason several batches were combined to derive the desired product in adequate quantities. For example, from 3.48 g combined **7**, 1.69 g **9** were obtained, and from 5.2 g combined **8**, 2.4 g **10** were obtained (48% and 46% yield for **9** and **10**, respectively) as crude material for further purification.

Purification of 9: The crude material was then purified by HPLC with a Waters CSH C18 and MeCN:H₂O:NH₃ as the mobile phase, followed by chiral supercritical fluid chromatography (SFC) with a Lux iC5 column in 45:55 EtOH:CO₂ (0.2% NH₃) (Supporting Information). For the small scale 39.1 and 36.8 mg of the two enantiomers were obtained (3.75% and 3.53% yield, respectively). The combined scaled up material gave 263 and 238 mg (5.61% and 5.08% yield, respectively). The order the two enantiomers are reported is the order of elution. The first enantiomer had similar retention time to **D1** (Supporting Information).

Purification of 10: The crude material was then purified by achiral SFC with a Torus Diol column in 80:20 MeOH:CO₂ and then chiral chromatography with a Lux C3 column in 50:50 MeOH:CO₂ (Supporting Information). For the small scale 23.5 and 24.2 mg of the two enantiomers were obtained (3.73% and 3.84% yield, respectively). The combined scaled up material gave 341 and 349 mg (6.49% and 6.64% yield, respectively). The first enantiomer had similar retention time to **D2** (Supporting Information).

(1,2-*trans*)-6-(5-(Ethylsulfonyl)benzo[d]oxazol-2-yl)-1,2-dihydronaphthalene-1,2-diol (9**)**

mp 193-194 °C; ¹H NMR (500 MHz, MeOH-*d*₄) δ 8.27 (d, *J* = 1.9 Hz, 1H), 8.15 (dd, *J* = 8.0, 1.8 Hz, 1H), 7.99 (d, *J* = 1.8 Hz, 1H), 7.98 (dd, *J* = 8.6, 1.8 Hz, 1H), 7.92 (d, *J* = 8.5 Hz, 1H), 7.78 (dd, *J* = 8.0, 1.2 Hz, 1H), 6.58 (dd, *J* = 9.9, 2.3 Hz, 1H), 6.07 (dd, *J* = 9.8, 2.5 Hz, 1H), 4.77

(dd, $J = 10.5, 1.2$ Hz, 1H), 4.43 (dt, $J = 10.5, 2.4$ Hz, 1H), 3.30 (q, $J = 7.4$ Hz, 2H), 1.26 (t, $J = 7.4$ Hz, 3H); ^{13}C NMR (125.5 MHz, MeOH- d_4) δ 166.8, 155.2, 143.7, 143.7, 136.9, 135.1, 134.2, 128.2, 127.40, 127.37, 126.8, 126.7, 126.3, 121.5, 112.9, 75.5, 73.7, 51.6, 7.7; $[\alpha_D^{25}] - 68.8$ [c 0.1, MeOH].

(1,2-*trans*)-7-(5-(Ethylsulfonyl)benzo[*d*]oxazol-2-yl)-1,2-dihydronaphthalene-1,2-diol (10)
mp 200-202 °C; ^1H NMR (500 MHz, DMSO- d_6) δ 8.37 (d, $J = 1.5$ Hz, 1H), 8.29 (d, $J = 1.9$ Hz, 1H), 8.09 (dd, $J = 7.9, 1.9$ Hz, 1H), 8.08 (d, $J = 8.5$ Hz, 1H), 7.95 (dd, $J = 8.5, 1.9$ Hz, 1H), 7.37 (d, $J = 7.9$ Hz, 1H), 6.52 (dd, $J = 9.8, 2.3$ Hz, 1H), 6.08 (dd, $J = 9.8, 2.3$ Hz, 1H), 5.85 (s, 1H), 5.39 (s, 1H), 4.65 (d, $J = 10.8$ Hz, 1H), 4.32 (d, $J = 10.8$ Hz, 1H), 3.39 (q, $J = 7.4$ Hz, 2H), 1.13 (t, $J = 7.4$ Hz, 3H); ^{13}C NMR (125.5 MHz, DMSO- d_6) δ 164.7, 153.2, 142.0, 139.6, 136.7, 136.4, 135.4, 126.9, 126.7, 125.6, 125.3, 124.6, 124.1, 119.9, 112.0, 73.3, 71.9, 49.5, 7.2; $[\alpha_D^{25}] - 172.6$ [c 0.1, MeOH].

Catechol intermediate and further oxidation to (1,2-*trans*)-6-(5-(ethylsulfonyl)benzo[*d*]oxazol-2-yl)-1,2-dihydronaphthalene-1,2-diol

To a stirred solution of **5** (20.6 g, 58.3 mmol) in DMF (200 mL) under a N_2 atmosphere stabilised IBX (16.3, 58.3 mmol) was added portionwise at 0 °C. The resulting mixture was stirred at rt for 48 h and then water (1000 mL) was added. The mixture was filtered, basified with NaHCO_3 , filtered again and the precipitate was washed with water (3x100 mL), THF (2x100 mL) and Et_2O (18.2 g of **7a** were collected).

^1H NMR (400 MHz, DMSO- d_6) δ 8.49 (s, 1H), 8.38 (d, $J = 1.3$ Hz, 1H), 8.37-8.33 (m, 1H), 8.20-8.15 (m, 1H), 8.14 (dd, $J = 8.6, 0.6$ Hz, 1H), 8.02 (dd, $J = 8.6, 1.8$ Hz, 1H), 7.88 (m, 1H), 6.52 (d, $J = 10.1$ Hz, 1H), 3.41 (q, $J = 7.3$ Hz, 2H), 1.14 (t, $J = 7.3$ Hz, 3H). LCMS (ESI+) 370.1 $[\text{M}+\text{H}]^+$, (ESI-) 368.1 $[\text{M}+\text{H}]^-$.

To a solution of **7a** (5.00 g, approx. 13.5 mmol) in DMF (10 mL) tetrachloro-*o*-benzoquinone (8.65 g, 35.2 mmol) was added under a N₂ atmosphere and the resulting mixture was stirred under room temperature for 24 h. The mixture was then poured into water (100 mL) and the precipitate was collected by filtration and washed with water (4.64 g, 79%). Spectroscopic data were identical to **7**.

Supporting Information.

Supporting Information is available free of charge on the ACS Publication website

Additional tables, figures, schemes, graphs and experimental procedures (pdf)

Copies of NMR spectra (pdf)

AUTHOR INFORMATION

Corresponding Author

Phone: +44 (0) 1865 275 643 (Chemistry)/271 883 (Pharmacology); e-mail:

angela.russell@chem.ox.ac.uk

Author Contributions

The manuscript was written through contributions of all authors. All authors have given approval to the final version of the manuscript.

Funding Sources

The authors wish to thank Summit Therapeutics plc (M.C., E.E., A.F., J.R., N.W.), the Medical Research Council (EP/L016044/1, I.W.; 1501AV003/CA2, K.E.D.), the Engineering and Physical Sciences Research Council (EP/L016044/1, I.W.) and Duchenne UK (N.W.) for financial support.

Notes

The authors declare the following competing financial interest(s): D.E., S.H., N.R., J.M.T., F.X.W. are or were Summit Therapeutics plc employees or consultants at the time that the work was conducted.

ACKNOWLEDGMENT

The authors kindly acknowledge Synthesis Med Chem (UK) and Charnwood Molecular (UK) for the scale ups for synthetic DHD1 and DHD3, Cerep (USA) for performing the intrinsic clearance of ezutromid in microsomes of different species, the *in vitro* metabolite identification study for ezutromid in human liver microsomes, and the secondary pharmacology evaluation for metabolites D1 and D2, Cyprotex Discovery Ltd (UK) for CYP 450 phenotyping, induction and inhibition studies, as well as, UGT phenotyping and UGT inhibition, Covance Laboratories Ltd (UK) for the *in vivo* radiochemical metabolite identification study for ezutromid in mice, the 28 day study in rat, and the 39 week study in minipig, Reach Separations Ltd. (UK) for the chiral separations and determination of chemical and chiral purity, Albany Molecular Research Inc. (AMRI®, USA) for the study of the *in vitro* production of dihydrodiol metabolites with MicroCyp® enzymes, recombinant human cytochrome P450 and a microbial biocatalyst panel, Absorption Systems for the study of biomimetic generation of dihydrodiols in human liver microsomes, XenoGesis Ltd (UK) for the production of the dihydrodiols by induced rat S9, Q² Solutions for metabolite structure determination/verification studies, Evotec (France) for performing the HTRF measurements, Evotec (UK) for physicochemical and ADME evaluation and SOLVO Biotechnology for the transporter interactions studies.

ABBREVIATIONS

ADMET, administration distribution metabolism excretion toxicity; BCRP, breast cancer resistance protein; BSEP, bile salt export pump; CYP, cytochrome P450; DHD, 1,2-dihydrodiol; DMD, Duchenne muscular dystrophy; EH, epoxide hydrolase; EMA, European Medicines Agency; EROD, 7-ethoxyresorufin-O-deethylase; FDA, Food and Drug Administration; HLM, human liver microsomes; HMBC, ^1H - ^{13}C heteronuclear multiple bond correlation; HSQC, ^1H - ^{13}C heteronuclear single quantum correlation; HTRF, homogenous time-resolved fluorescence; KinSol, kinetic solubility; MAO, monoamino oxidase; MATE, multidrug and toxic compound extrusion; MDR, multidrug resistant; NOESY, nuclear Overhauser effect spectroscopy; OCT, organic cation transporter; OATP, organic anion transporter protein; PAMPA, parallel artificial membrane permeability assay; PPB, plasma protein binding; PROD, 7-pentoxoresorufin O-depethylase; PD, pharmacodynamics; PK, pharmacokinetics; TDO, toluene dioxygenase; UGT, uridine glucuronyl transferase.

REFERENCES

1. Emery, A. E., Population frequencies of inherited neuromuscular diseases -a world survey. *Neuromuscul. Disord.* **1991**, *1*, 19-29.
2. van Deutekom, J. C.; van Ommen, G. J., Advances in Duchenne muscular dystrophy gene therapy. *Nat. Rev. Genet.* **2003**, *4*, 774-783.
3. Blake, D. J.; Weir, A.; Newey, S. E.; Davies, K. E., Function and genetics of dystrophin and dystrophin-related proteins in muscle. *Physiol. Rev.* **2002**, *82*, 291-329.
4. Hoffman, E. P.; Brown, R. H., Jr.; Kunkel, L. M., Dystrophin: the protein product of the Duchenne muscular dystrophy locus. *Cell* **1987**, *51*, 919-928.
5. Guiraud, S.; Davies, K. E., Pharmacological advances for treatment in Duchenne muscular dystrophy. *Curr. Opin. Pharmacol.* **2017**, *34*, 36-48.
6. Love, D. R.; Hill, D. F.; Dickson, G.; Spurr, N. K.; Byth, B. C.; Marsden, R. F.; Walsh, F. S.; Edwards, Y. H.; Davies, K. E., An autosomal transcript in skeletal muscle with homology to dystrophin. *Nature* **1989**, *339*, 55-58.
7. Deconinck, N.; Tinsley, J.; De Backer, F.; Fisher, R.; Kahn, D.; Phelps, S.; Davies, K.; Gillis, J. M., Expression of truncated utrophin leads to major functional improvements in dystrophin-deficient muscles of mice. *Nat. Med.* **1997**, *3*, 1216-1221.

8. Tinsley, J.; Deconinck, N.; Fisher, R.; Kahn, D.; Phelps, S.; Gillis, J. M.; Davies, K., Expression of full-length utrophin prevents muscular dystrophy in mdx mice. *Nat. Med.* **1998**, *4*, 1441-1444.
9. Cerletti, M.; Negri, T.; Cozzi, F.; Colpo, R.; Andreetta, F.; Croci, D.; Davies, K. E.; Cornelio, F.; Pozza, O.; Karpati, G.; Gilbert, R.; Mora, M., Dystrophic phenotype of canine X-linked muscular dystrophy is mitigated by adenovirus-mediated utrophin gene transfer. *Gene Ther.* **2003**, *10*, 750-757.
10. Wynne, G. M.; Russell, A. J., Drug Discovery Approaches for Rare Neuromuscular Diseases. In *Orphan Drugs and Rare Diseases*, The Royal Society of Chemistry: 2014; pp 257-343.
11. Guiraud, S.; Roblin, D.; Kay, D. E., The potential of utrophin modulators for the treatment of Duchenne muscular dystrophy. *Expert Opin. Orphan Drugs* **2018**, *6*, 179-192.
12. http://otp.investis.com/clients/uk/summit_corporation_plc/rns/regulatory-story.aspx?newsid=1084945&cid=1575
13. Tinsley, J.; Robinson, N.; Davies, K. E., Safety, tolerability, and pharmacokinetics of SMT C1100, a 2-arylbenzoxazole utrophin modulator, following single- and multiple-dose administration to healthy male adult volunteers. *J. Clin. Pharmacol.* **2015**, *55*, 698-707.
14. Ricotti, V.; Spinty, S.; Roper, H.; Hughes, I.; Tejura, B.; Robinson, N.; Layton, G.; Davies, K.; Muntoni, F.; Tinsley, J., Safety, Tolerability, and Pharmacokinetics of SMT C1100, a 2-Arylbenzoxazole Utrophin Modulator, following Single- and Multiple-Dose Administration to Pediatric Patients with Duchenne Muscular Dystrophy. *PLoS One* **2016**, *11*, e0152840.
15. Muntoni, F.; Tejura, B.; Spinty, S.; Roper, H.; Hughes, I.; Layton, G.; Davies, K. E.; Harriman, S.; Tinsley, J., A Phase 1b Trial to Assess the Pharmacokinetics of Ezutromid in Pediatric Duchenne Muscular Dystrophy Patients on a Balanced Diet. *Clin. Pharmacol. Drug Dev.* **2019**, Accepted manuscript, <https://doi.org/10.1002/cpdd.642>.
16. Jerina, D. M.; Daly, J. W.; Witkop, B.; Zaltzman-Nirenberg, P.; Udenfriend, S., The role of arene oxide-oxepin systems in the metabolism of aromatic substrates. 3. Formation of 1,2-naphthalene oxide from naphthalene by liver microsomes. *J. Am. Chem. Soc.* **1968**, *90*, 6525-6527.
17. Jerina, D. M.; Daly, J. W.; Witkop, B.; Zaltzman-Nirenberg, P.; Udenfriend, S., 1,2-naphthalene oxide as an intermediate in the microsomal hydroxylation of naphthalene. *Biochemistry* **1970**, *9*, 147-156.
18. Doherty, M. A.; Makowski, R.; Gibson, G. G.; Cohen, G. M., Cytochrome P-450 dependent metabolic activation of 1-naphthol to naphthoquinones and covalent binding species. *Biochem. Pharmacol.* **1985**, *34*, 2261-2267.
19. Wilson, A. S.; Davis, C. D.; Williams, D. P.; Buckpitt, A. R.; Pirmohamed, M.; Park, B. K., Characterisation of the toxic metabolite(s) of naphthalene. *Toxicology* **1996**, *114*, 233-242.
20. Cho, T. M.; Rose, R. L.; Hodgson, E., In vitro metabolism of naphthalene by human liver microsomal cytochrome P450 enzymes. *Drug Metab. Dispos.* **2006**, *34*, 176-183.
21. Genter, M. B.; Marlowe, J.; Kevin Kerzee, J.; Dragin, N.; Puga, A.; Dalton, T. P.; Nebert, D. W., Naphthalene toxicity in mice and aryl hydrocarbon receptor-mediated CYPs. *Biochem. Biophys. Res. Commun.* **2006**, *348*, 120-123.
22. Tingle, M. D.; Pirmohamed, M.; Templeton, E.; Wilson, A. S.; Madden, S.; Kitteringham, N. R.; Park, B. K., An investigation of the formation of cytotoxic, genotoxic, protein-reactive and stable metabolites from naphthalene by human liver microsomes. *Biochem. Pharmacol.* **1993**, *46*, 1529-1538.

23. Kumar, G. N.; Sproul, C.; Poppe, L.; Turner, S.; Gohdes, M.; Ghoborah, H.; Padhi, D.; Roskos, L., Metabolism and disposition of calcimimetic agent cinacalcet HCl in humans and animal models. *Drug Metab. Dispos.* **2004**, *32*, 1491-1500.
24. Risch, P.; Pfeifer, T.; Segrestaa, J.; Fretz, H.; Pothier, J., Verification of the Major Metabolic Oxidation Path for the Naphthoyl Group in Chemoattractant Receptor-Homologous Molecule Expressed on Th2 Cells (CRTh2) Antagonist 2-(2-(1-Naphthoyl)-8-fluoro-3,4-dihydro-1H-pyrido[4,3-b]indol-5(2H)-yl)acetic Acid (Setipiprant/ACT-129968). *J. Med. Chem.* **2015**, *58*, 8011-8035.
25. Hoch, M.; Wank, J.; Kluge, I.; Wagner-Redeker, W.; Dingemanse, J., Disposition and metabolism of setipiprant, a selective oral CRTH2 antagonist, in humans. *Drugs R. D.* **2013**, *13*, 253-269.
26. Vickers, A. E.; Sinclair, J. R.; Zollinger, M.; Heitz, F.; Glanzel, U.; Johanson, L.; Fischer, V., Multiple cytochrome P-450s involved in the metabolism of terbinafine suggest a limited potential for drug-drug interactions. *Drug Metab. Dispos.* **1999**, *27*, 1029-1038.
27. Gennaro, P. D.; Galli, E.; Albini, G.; Pelizzoni, F.; Sello, G.; Bestetti, G., Production of substituted naphthalene dihydrodiols by engineered *Escherichia coli* containing the cloned naphthalene 1,2-dioxygenase gene from *Pseudomonas fluorescens* N3. *Res. Microbiol.* **1997**, *148*, 355-364.
28. Shindo, K.; Osawa, A.; Kasai, Y.; Iba, N.; Saotome, A.; Misawa, N., Hydroxylations of substituted naphthalenes by *Escherichia coli* expressing aromatic dihydroxylating dioxygenase genes from polycyclic aromatic hydrocarbon-utilizing marine bacteria. *J. Mol. Catal. B Enzym.* **2007**, *48*, 77-83.
29. Whited, G. M.; Downie, J. C.; Hudlicky, T.; Fearnley, S. P.; Dudding, T. C.; Olivo, H. F.; Parker, D., Oxidation of 2-methoxynaphthalene by toluene, naphthalene and biphenyl dioxygenases: structure and absolute stereochemistry of metabolites. *Bioorg. Med. Chem.* **1994**, *2*, 727-734.
30. Bestetti, G.; Bianchi, D.; Bosetti, A.; Di Gennaro, P.; Galli, E.; Leoni, B.; Pelizzoni, F.; Sello, G., Bioconversion of substituted naphthalenes to the corresponding 1,2-dihydro-1,2-dihydroxy derivatives. Determination of the regio- and stereochemistry of the oxidation reactions. *Appl. Microbiol. Biotechnol.* **1995**, *44*, 306-313.
31. Hudlicky, T.; Endoma, M. A. A.; Butora, G., New chiral synthons from the microbial oxidation of bromonaphthalenes. *Tetrahedron: Asymmetry* **1996**, *7*, 61-68.
32. Kwit, M.; Gawronski, J.; Boyd, D. R.; Sharma, N. D.; Kaik, M.; More O'Ferrall, R. A.; Kudavalli, J. S., Toluene dioxygenase-catalyzed synthesis of cis-dihydrodiol metabolites from 2-substituted naphthalene substrates: assignments of absolute configurations and conformations from circular dichroism and optical rotation measurements. *Chem. Eur. J.* **2008**, *14*, 11500-11511.
33. Tsui, G. C.; Lautens, M., Rhodium(I)-catalyzed domino asymmetric ring opening/enantioselective isomerization of oxabicyclic alkenes with water. *Angew. Chem. Int. Ed.* **2012**, *51*, 5400-5404.
34. Mukherjee, P.; Roy, S. J.; Sarkar, T. K., A diversity-oriented synthesis of bicyclic cis-dihydroarenediols, cis-4-hydroxyscytalones, and bicyclic conduritol analogues. *Org. Lett.* **2010**, *12*, 2472-2475.
35. Olesen, O. V.; Linnet, K., Identification of the human cytochrome P450 isoforms mediating in vitro N-dealkylation of perphenazine. *Br. J. Clin. Pharmacol.* **2000**, *50*, 563-571.

36. Dierks, E. A.; Stams, K. R.; Lim, H. K.; Cornelius, G.; Zhang, H.; Ball, S. E., A method for the simultaneous evaluation of the activities of seven major human drug-metabolizing cytochrome P450s using an in vitro cocktail of probe substrates and fast gradient liquid chromatography tandem mass spectrometry. *Drug Metab. Dispos.* **2001**, 29, 23-29.
37. Donato, M. T.; Gomez-Lechon, M. J.; Castell, J. V., A microassay for measuring cytochrome P450IA1 and P450IIB1 activities in intact human and rat hepatocytes cultured on 96-well plates. *Anal. Biochem.* **1993**, 213, 29-33.
38. Skaanild, M. T.; Friis, C., Cytochrome P450 sex differences in minipigs and conventional pigs. *Pharmacol. Toxicol.* **1999**, 85, 174-180.
39. Tinsley, J. M.; Fairclough, R. J.; Storer, R.; Wilkes, F. J.; Potter, A. C.; Squire, S. E.; Powell, D. S.; Cozzoli, A.; Capogrosso, R. F.; Lambert, A.; Wilson, F. X.; Wren, S. P.; De Luca, A.; Davies, K. E., Daily treatment with SMTc1100, a novel small molecule utrophin upregulator, dramatically reduces the dystrophic symptoms in the mdx mouse. *PLoS One* **2011**, 6, e19189.

For Table of Contents Only

